

邊界元素法求解內域假根與外域虛擬波數的理論探討與數值研究

Analytical study and numerical experiments for spurious eigensolutions of interior problem and the fictitious wave number of exterior acoustic problem using BEM

陳正宗¹，陳義麟²，陳桂鴻³

Keywords: spurious eigenvalue, real-part BEM, fictitious frequency, circulant, degenerate kernels

Abstract

In this report the reason why the spurious solution occurs in the interior eigenproblem using real-part BEM and why the fictitious solution occurs in numerical computations of the exterior Helmholtz integral equation at certain characteristic frequencies is investigated. It was recently found that the real-part BEM for the interior problem results in spurious eigensolutions. The real-part BEM results in spurious solutions for interior problems in a similar way that the singular integral equation results in fictitious solutions for the exterior problem. Both the two problems stem from the rank deficiency of the influence matrix. By using the circulant properties and degenerate kernels, an analytical scheme in a discrete system of a circular case is achieved. Numerical experiments are found to agree with the analytical results.

¹ 國立台灣海洋大學河海工程學系教授

² 國立高雄海洋技術學院造船工程科副教授

³ 國立台灣海洋大學河海工程學系研究生

1、 INTRODUCTION

Acoustic problems are generally modeled using the wave equation. While the solution to the original boundary value problem in the domain exterior to the boundary is perfectly unique for all wave numbers, this is not the case for the corresponding integral equation formulation, which breaks down at certain frequencies known as irregular frequencies or fictitious frequencies. This problem is completely nonphysical because there are no eigenvalues for the exterior problems. Schenck [1] proposed a CHIEF (Combined Helmholtz Interior integral Equation Formulation) method, which is easy to implement and is efficient but still has some drawbacks. Burton and Miller [2] proposed an integral equation that was valid for all wave numbers by forming a linear combination of the singular integral equation and its normal derivative. In the case of a fictitious frequency, the resulting coefficient matrix for the exterior acoustic problems becomes singular or ill-conditioned. This means that the boundary integral equations are not linearly independent and the matrix is rank deficient. In the fictitious-frequency case, the rank of the coefficient matrix is less than $2N$, where $2N$ is the number of boundary elements. The SVD (Singular Value Decomposition) technique can be employed to detect the fictitious frequency by checking whether or not the minimum singular value, S_1 is zero.

For interior problems, eigensolutions are often encountered not only in vibration problems but also in acoustics. Based on the complex-valued boundary element method (BEM) [3], the eigenvalues and eigenmodes can be determined. Nevertheless, complex-valued computation is required. To avoid complex-valued computation the MRM approach has been proposed. In the other hand, Tai and Shaw [4] employed only real-part kernels to solve the eigenproblem. A simplified method using only the real-part or imaginary-part kernel was also presented by De Mey [5]. Although De Mey found that the zeros for a real-part determinant may be different from those for imaginary-part determinant, the spurious solutions were not discovered. Kang *et al.* [6] employed the nondimensional dynamic influence function method to solve the eigenproblem. Chen *et al.* [7] commented that NDIF method is a special case of imaginary-part BEM. The reason why spurious eigenvalues occur in the real-part BEM is the loss of the constraints, which was investigated by Yieh *et al.* [8]. The fewer number of constraint equations makes the solution space larger. The spurious eigensolutions can be filtered out using many alternatives: *e.g.*, the complex valued formulation, the domain partition technique, the dual formulation in conjunction with SVD [9] and the CHEEF (Combined Helmholtz Exterior integral Equation Formulation) method [10].

Based on the circulant properties and degenerate kernels, the reason why the fictitious wave number and spurious eigensolution occur can be easily understood. We explore the mechanism of them and found the relationship between the spurious eigenvalue (interior problem) and fictitious frequency (exterior problem).

2、AN UNIFIED FORMULATION FOR HELMHOLTZ INTERIOR AND EXTERIOR PROBLEMS

The governing equation is the Helmholtz equation as follows:

$$(\nabla^2 + k^2)u(x_1, x_2) = 0, \quad (x_1, x_2) \in D, \quad (1)$$

where ∇^2 is the Laplacian operator, D can be D^i for interior problem and D can be D^e for exterior problem and k is the wave number, which is angular frequency over the speed of sound. The unified integral formulation for the Helmholtz equation can be written as

$$0 = \int_B T(s, x)u(s)dB(s) - \int_B U(s, x)t(s)dB(s), \quad (2)$$

$$0 = \int_B M(s, x)u(s)dB(s) - \int_B L(s, x)t(s)dB(s), \quad (3)$$

where $t(s) = \frac{\partial u(s)}{\partial n_s}$ and $L(s, x) = \frac{\partial U(s, x)}{\partial n_x}$, $M(s, x) = \frac{\partial^2 U(s, x)}{\partial n_s \partial n_x}$, B denotes the boundary enclosing D and

$U = U^i(s, x)$, $T = T^i(s, x)$, for exterior problem, and $U = U^e(s, x)$, $T = T^e(s, x)$, for interior problem.

The kernels of U^i , U^e , T^i , and T^e can be derived from multipole expansion and the explicit forms of the four kernels will be elaborated on later.

3、ANALYTICAL STUDY FOR THE SPURIOUS AND FICTITIOUS SOLUTIONS USING DEGENERATE KERNELS AND CIRCULANTS

By using the two bases of first and second-kind Bessel functions, $J_m(kx)$ and $Y_m(kx)$, we can decompose the kernel functions into

$$U(s, x) = \begin{cases} U^i(\mathbf{q}) = \sum_{n=-\infty}^{\infty} \frac{\mathbf{P}}{2} [-iJ_n(kR) + Y_n(kR)] J_n(k\mathbf{r}) \cos(n\mathbf{q}), R > \mathbf{r} \\ U^e(\mathbf{q}) = \sum_{n=-\infty}^{\infty} \frac{\mathbf{P}}{2} [-iJ_n(k\mathbf{r}) + Y_n(k\mathbf{r})] J_n(kR) \cos(n\mathbf{q}), R < \mathbf{r} \end{cases} \quad (4)$$

$$T(s, x) = \begin{cases} T^i(\mathbf{q}) = \sum_{n=-\infty}^{\infty} \frac{k\mathbf{P}}{2} [-iJ'_n(kR) + Y'_n(kR)] J_n(k\mathbf{r}) \cos(n\mathbf{q}), R > \mathbf{r} \\ T^e(\mathbf{q}) = \sum_{n=-\infty}^{\infty} \frac{k\mathbf{P}}{2} [-iJ_n(k\mathbf{r}) + Y_n(k\mathbf{r})] J'_n(kR) \cos(n\mathbf{q}), R < \mathbf{r} \end{cases} \quad (5)$$

$$L(s, x) = \begin{cases} L^i(\mathbf{q}) = \sum_{n=-\infty}^{\infty} \frac{k\mathbf{p}}{2} [-iJ_n(kR) + Y_n(kR)] J_n'(k\mathbf{r}) \cos(n\mathbf{q}), R > r \\ L^e(\mathbf{q}) = \sum_{n=-\infty}^{\infty} \frac{k\mathbf{p}}{2} [-iJ_n'(k\mathbf{r}) + Y_n'(k\mathbf{r})] J_n(kR) \cos(n\mathbf{q}), R < r \end{cases} \quad (6)$$

$$M(s, x) = \begin{cases} M^i(\mathbf{q}) = \sum_{n=-\infty}^{\infty} \frac{k^2\mathbf{p}}{2} [-iJ_n'(kR) + Y_n'(kR)] J_n'(k\mathbf{r}) \cos(n\mathbf{q}), R > r \\ M^e(\mathbf{q}) = \sum_{n=-\infty}^{\infty} \frac{k^2\mathbf{p}}{2} [-iJ_n(k\mathbf{r}) + Y_n(k\mathbf{r})] J_n'(kR) \cos(n\mathbf{q}), R < r \end{cases} \quad (7)$$

where x is specified by $(\mathbf{r}, 0)$ in polar coordinate. The definitions of \mathbf{r} , R and \mathbf{q} for interior and exterior problems are shown in Fig.1 and Fig.2, respectively. Based on the circulants for the finite d.o.f. system by discretizing $2N$ constant elements, we have

$$[G] = \begin{bmatrix} a_0 & a_1 & \cdots & a_{2N-2} & a_{2N-1} \\ a_{2N-1} & a_0 & \cdots & a_{2N-3} & a_{2N-2} \\ \vdots & \cdots & \ddots & \vdots & \vdots \\ a_1 & a_2 & \cdots & a_{2N-1} & a_0 \end{bmatrix} \quad (8)$$

where

$$a_m = \int_{(m-1/2)\Delta\mathbf{q}}^{(m+1/2)\Delta\mathbf{q}} G(\mathbf{q}) R d\mathbf{q} \approx G(\mathbf{q}_m) R \Delta\mathbf{q} \quad (9)$$

where $m = 0, 1, \dots, 2N-1$ and $G(\mathbf{q})$ can be $U^i, U^e, T^i, T^e, L^i, L^e, M^i$ and M^e . By using the similar properties for all the eight matrices with respect to circulant, we have

$$\det[U^i] = \mathbf{I}_0 \mathbf{I}_N (\mathbf{I}_1 \cdots \mathbf{I}_{N-1}) (\mathbf{I}_{-1} \cdots \mathbf{I}_{-(N-1)}) \quad (10)$$

$$\det[U^e] = \mathbf{I}_0 \mathbf{I}_N (\mathbf{I}_1 \cdots \mathbf{I}_{N-1}) (\mathbf{I}_{-1} \cdots \mathbf{I}_{-(N-1)}) \quad (11)$$

$$\det[T^e] = \mathbf{m}_0 \mathbf{m}_N (\mathbf{I} \mathbf{m} \cdots \mathbf{m}_{N-1}) (\mathbf{m}_{-1} \cdots \mathbf{m}_{-(N-1)}) \quad (12)$$

$$\det[L^i] = \mathbf{m}_0 \mathbf{m}_N (\mathbf{I} \mathbf{m} \cdots \mathbf{m}_{N-1}) (\mathbf{m}_{-1} \cdots \mathbf{m}_{-(N-1)}) \quad (13)$$

$$\det[T^i] = \mathbf{u}_0 \mathbf{u}_N (\mathbf{u}_1 \cdots \mathbf{u}_{N-1}) (\mathbf{u}_{-1} \cdots \mathbf{u}_{-(N-1)}) \quad (14)$$

$$\det[L^e] = \mathbf{u}_0 \mathbf{u}_N (\mathbf{u}_1 \cdots \mathbf{u}_{N-1}) (\mathbf{u}_{-1} \cdots \mathbf{u}_{-(N-1)}) \quad (15)$$

$$\det[M^i] = k_0 k_N (k_1 \cdots k_{N-1}) (k_{-1} \cdots k_{-(N-1)}) \quad (16)$$

$$\det[M^e] = k_0 k_N (k_1 \cdots k_{N-1}) (k_{-1} \cdots k_{-(N-1)}) \quad (17)$$

where

$$\mathbf{I}_l = \mathbf{p}^2 \mathbf{r} (-iJ_l(k\mathbf{r}) + Y_l(k\mathbf{r})) J_l(k\mathbf{r}), \quad (18)$$

$$\mathbf{m}_l = \mathbf{p}^2 k\mathbf{r} (-iJ_l'(k\mathbf{r}) + Y_l'(k\mathbf{r})) J_l(k\mathbf{r}), \quad (19)$$

$$\mathbf{u}_l = \mathbf{p}^2 k\mathbf{r} (-iJ_l(k\mathbf{r}) + Y_l(k\mathbf{r})) J_l'(k\mathbf{r}), \quad (20)$$

$$\mathbf{v}_l = \mathbf{p}^2 k\mathbf{r} (-iJ_l'(k\mathbf{r}) + Y_l'(k\mathbf{r})) J_l'(k\mathbf{r}), \quad (21)$$

and $l = 0, \pm 1, \pm 2, \dots \pm (N-1), N$.

For the exterior radiation problem, considering the Dirichlet radiation problem, *i.e.*, $u(x) = \bar{u}$ is considered. Therefore, we obtain the following equation,

$$[U]\{t\} = [\bar{T}]\{\bar{u}\}. \quad (22)$$

Based on Eqs. (18) and (22), the possible fictitious frequencies occur at the position k which satisfies

$$(-iJ_l(k\mathbf{r}) + Y_l(k\mathbf{r}))J_l(k\mathbf{r}) = 0 \quad (23)$$

Since $(-iJ_l(k\mathbf{r}) + Y_l(k\mathbf{r}))$ is never zero, the k value satisfying Eq.(23), implies

$$J_l(k\mathbf{r}) = 0. \quad (24)$$

Schenck used the CHIEF method, which employs the boundary integral equations by collocating the interior point as an auxiliary condition to make up deficient constraint condition. Combination of the integral equations for the boundary points and those in the interior points yields the over-determined equation system,

$$\begin{bmatrix} U_{2N \times 2N}^B \\ U_a^i \end{bmatrix} \{t\} = \begin{bmatrix} \bar{T}_{2N \times 2N}^B \\ T_a^i \end{bmatrix} \{\bar{u}\} \quad (25)$$

where the superscript B denotes the boundary, the subscript i denotes the interior domain and a is the number of additional points. Chen *et al.* [11] suggested the optimum numbers and proper positions for the collocation points in the interior domain by using analytical study and numerical experiments.

Burton and Miller proposed an integral equation by combining the singular integral equation and its normal derivative,

$$[U + \frac{i}{k}L]\{t\} = [T + \frac{i}{k}M]\{\bar{u}\}. \quad (26)$$

Eq.(26) was valid for all wave numbers.

For the interior Dirichlet problem, the complex-valued UT and LM formulation can obtain the eigenequations

$$(J_l(k\mathbf{r}) + iY_l(k\mathbf{r}))J_l(k\mathbf{r}) = 0 \quad (27)$$

and

$$(-iJ_l'(k\mathbf{r}) + Y_l'(k\mathbf{r}))J_l(k\mathbf{r}) = 0. \quad (28)$$

Since $(J_l(k\mathbf{r}) + iY_l(k\mathbf{r}))$ and $(J_l'(k\mathbf{r}) + iY_l'(k\mathbf{r}))$ are never zero, the true eigenvalues are the roots of $J_l(k\mathbf{r}) = 0$ for both UT and LM equations.

By employing the real-part UT equation (18), we obtain the eigenequation,

$$Y_l(k\mathbf{r})J_l(k\mathbf{r}) = 0, \quad l = 0, \pm 1, \dots \pm (N-1), N. \quad (29)$$

The k values satisfying Eq.(29) may be spurious eigenvalue ($Y_l(k\mathbf{r})=0$) or true eigenvalue ($J_l(k\mathbf{r})=0$). If we employ the real-part *LM* equation (19), we obtain the eigenequation

$$Y'_l(k\mathbf{r})J_l(k\mathbf{r}) = 0, \quad l = 0, \pm 1, \dots \pm (N-1), N. \quad (30)$$

The k values satisfying Eq.(30) may be spurious eigenvalue ($Y'_l(k\mathbf{r})=0$) or true eigenvalue ($J_l(k\mathbf{r})=0$). After comparing Eqs.(29) and (30) with Eqs.(18) and (19), it can be realized that the reason why spurious eigenvalues occur is due to the loss of constraints in the imaginary-part information. Chen *et al.* [10] proposed the CHEEF method by combining the integral equations for the boundary points and those in the exterior points. It yields the over-determined equation system,

$$\begin{bmatrix} U_{2N \times 2N}^B \\ U_a^e \end{bmatrix} \{t\} = 0, \quad (31)$$

where the subscript e denotes the exterior domain. It can filter out the spurious eigensolutions efficiently.

4、 NUMERICAL EXAMPLES

Case 1. Fictitious frequency for exterior problem

For the exterior acoustic problem, we consider the Neumann problem (nonuniform radiation of an infinite circular cylinder $a=1.0m$). This problem was chosen because the exact solution is known [12]. In this example we computed the nonuniform radiation of an infinite circular cylinder. The Neumann boundary condition is applied to the cylinder surface. The portion ($-a < q < a$) is assigned a unit value, while the remaining portion is assigned a homogeneous value. The exact solution is given by

$$u(r, \mathbf{q}) = -\frac{2}{p} \sum_{n=1}^{\infty} \frac{\sin(n\mathbf{q})}{n} \frac{H_n^{(1)}(kr)}{H_n^{(1)}(ka)} \cos n\mathbf{q}, \quad r > a, 0 < \mathbf{q} < 2p,$$

where $H_n^{(1)}$ and $H_n^{(1) \prime}$ denotes the first kind Hankel function with order n and its derivative, respectively. Thirty-two elements are adopted in the BEM mesh and $a = 5p/32$ for this case. Using the singular (*UT*) equation, the positions where the irregular values occur can be found in Fig.3 for the solution $u(a, 0; k)$ versus k . It is found that irregular values occur at the positions of $J_{n,m}$, which is the m th zero of $J_n(ka)$. It agrees well as predicted in Eq.(24). Fig.4 show the solution $u(a, 0; k)$ versus k using the *LM* equation, the positions where the irregular values occur at the positions of $J_{n,m}'$, which is the m -th zero of $J_n'(ka)$. Fig.5 shows the solution $u(a, 0; k)$ versus k using the Burton and Miller approach. Fig.6 show the solution $u(a, 0; k)$ versus k using the CHIEF method.

Both of these methods can avoid the nonunique problem.

Case 2. Spurious eigensolution for interior problem

For the numerical experiment, we considered a circular cavity with a radius 1.0 m subjected to the Dirichlet boundary condition. Fig.7 shows the minimum singular value, s_1 , versus k , where the true and spurious eigenvalues are obtained if only real-part UT equation is used. In the range of $0 < k < 5$, we have two true eigenvalues ($J_{0,1}(2.405)$ and $J_{1,1}(3.832)$) and five spurious eigenvalues ($Y_{0,1}(0.894)$, $Y_{1,1}(2.197)$, $Y_{2,1}(3.384)$, $Y_{0,2}(3.958)$ and $Y_{3,1}(4.527)$). It agrees well as predicted in Eq.(29). Fig.8 shows the ill-posed behavior [13], since only imaginary-part UT equation is used. Theoretically speaking, we can obtain the true and spurious eigenvalues [14], but the coefficient matrix is ill-posed in numerical computation. Fig.9 shows the absolute value of determinant using the complex UT equation, only true eigenvalues are obtained. Fig.10 shows the first minimum singular value, s_1 , versus k , where only the true eigenvalues are obtained using the CHEEF method.

5、 CONCLUSIONS

In this report, the mechanism of fictitious frequency and spurious eigenvalue were investigated using the degenerate kernels and circulants for a discrete system of a circle. The reason why spurious eigenvalues occur in the real-part BEM and why fictitious frequencies results from the rank deficiency of influence matrix were explained. The numerical results agree well with the analytical prediction using circulants in the circular case. The relationship between interior eigensolution problem and exterior fictitious frequency problem are summarized in Table 1.

7、 Acknowledgement

Financial support from the National Science Council, Grant No. NSC-89-2211-E-019-003, to National Taiwan Ocean University is gratefully acknowledged.

6、 REFERENCES

- [1] H. A. Schenck, *Improved integral formulation for acoustic radiation problems*, J. Acoust. Soc. Am. **44**(1), 41-58 1968.
- [2] A. J. Burton and G. F. Miller, *The application of integral equation methods to numerical*

- solutions of some exterior boundary value problem*. Proc. of the Royal Society London Ser A **323**, 201-210. 1971.
- [3] D. Y. Liou, J. T. Chen and K. H. Chen, *A new method for determining the acoustic modes of a two-dimensional sound field*, J. Chinese Inst. Civ. Hydr. Engng., **11**(2), 89-100, 1999. (in Chinese)
- [4] G. R. G. Tai and R. P. Shaw, *Helmholtz equation eigenvalues and eigenmodes for arbitrary domains*, Journal of the Acoustical Society of America., **56**, 796-804, 1974.
- [5] G. De Mey, *A simplified integral equation method for the calculation of the eigenvalues of Helmholtz equation*, Int. J. Numer. Meth. Engng., **11**, 1340-1342 1977.
- [6] S. W. Kang, J. M. Lee and Y. J. Kang, *Vibration analysis of arbitrarily shaped membranes using non-dimensional dynamic influence function*, Journal of Sound and Vibration, **221**(1), 117-132, 1999.
- [7] J. T. Chen, S. R. Kuo, K. H. Chen and Y. C. Cheng, *Comments on vibration analysis of arbitrary shaped membranes using nondimensional dynamic influence function*, Journal of Sound and Vibration, **234**(1), 156-171, 2000.
- [8] W. Yieh, J. T. Chen, K. H. Chen and F. C. Wong, *A study on the multiple reciprocity method and complex-valued formulation for the Helmholtz equation*, Adv. Engng. Soft., **29** (1), 1-6 1997.
- [9] J. T. Chen, C. X. Huang and F. C. Wong *Determination of spurious eigenvalues and multiplicities of true eigenvalues in the dual multiple reciprocity method using the singular value decomposition technique*. Journal of Sound and Vibration, **230**(2), 203-219. 2000.
- [10] I. L. Chen, J. T. Chen, S. R. Kuo, and M. T. Liang, *A new method for true and spurious eigensolutions of arbitrary cavities using the CHEEF method*, J. Acoust. Soc. Amer., **109**(3), 982-999, 2001.
- [11] I. L. Chen, J. T. Chen and M. T. Liang, *Analytical study and numerical experiments for radiation and scattering problems using the CHIEF method*, Journal of Sound and Vibration, **248**(5), 809-828., 2001.
- [12] I. Harari, P. E. Barbone and J. M. Montgomery, *Finite element formulations for exterior problems: Application to hybrid methods, non-reflecting boundary conditions, and infinite elements*. International Journal for Numerical Methods in Engineering. **40**, 2791-2805. 1997.

- [13] S. R. Kuo, W. Yeih and Y. C. Wu, *Applications of the generalized singular-value decomposition method on the eigenproblem using the incomplete boundary element formulation*. Journal of Sound and Vibration. **235**(5), 813-845, 2000.
- [14] J. T. Chen, S. R. Kuo and K. H. Chen, *A nonsingular integral formulation for the Helmholtz eigenproblems of a circular domain*. Journal of the Chinese Institute of Engineers, **22**(6), 729-739, 1999.
- [15] J. T. Chen, C. T. Chen, K. H. Chen and I. L. Chen, *On fictitious frequencies using dual BEM for non-uniform radiation problems of a cylinder*, Mech. Res. Comm., Accepted, 2000.
- [16] S. R. Kuo, J. T. Chen and C. X. Huang, *Analytical study and numerical experiments for true and spurious eigensolutions of a circular cavity using the real-part BEM*, Int. J. Numer. Meth. Engng., **48** (9), 1401-1422, 2000.

關鍵詞：假特徵值，實部邊界元素法，虛擬頻率，圓形循環矩陣，退化核函數

中文摘要

本研究報告在於討論以積分方程求解內域或外域 Helmholtz 場在數值上產生的真假特徵值及虛擬頻率的問題。在解外域聲場時於某些特徵頻率會得到不唯一的解。而在求解內域特徵值時如果僅採用實部邊界元素法的奇異積分方程式，則會得到假特徵值。而內域實數邊界元素法得到假根與外域問題得到虛擬頻率的原因是類似的。兩個問題的產生皆由於影響矩陣的秩數不足所致。藉由圓形循環矩陣的特性及退化核函數，可得知為何採用實部邊界元素法會產生假根是因為少了虛數部的限制而產生了假根。而虛擬頻率(或波數)的產生則是數學上 $0/0$ 的問題。在解析上我們以二維圓形問題來證明，並以設計的數值實驗結果來驗證我們理論的正確性。

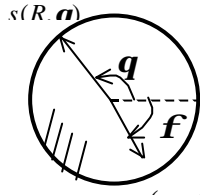


Fig.1 The definitions of $\mathbf{r}, \mathbf{q}, R$ and r , for $U^e(s, x)$ kernel.

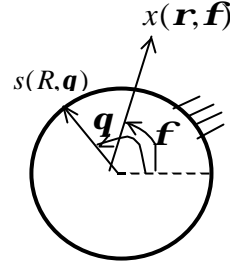


Fig.2 The definitions of $\mathbf{r}, \mathbf{q}, R$ and r , for $U^i(s, x)$ kernel.

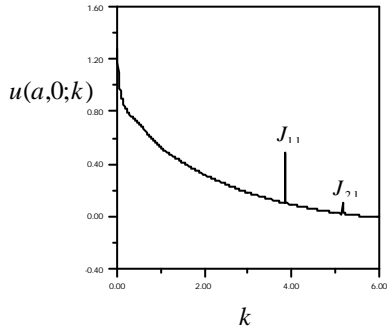


Fig.3 $u(a, 0; k)$ versus k using the UT method.

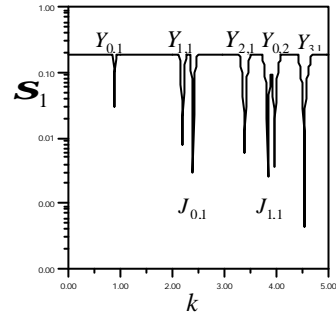


Fig.7 \mathbf{S}_1 versus k using the real-part BEM.

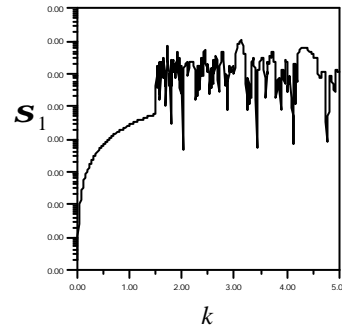
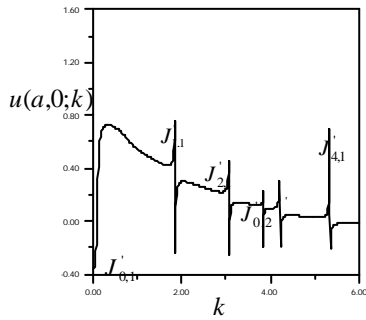


Fig.8 \mathbf{S}_1 versus k using the imaginary-part BEM

Fig.4 $u(a,0;k)$ versus k using
the *LM* method

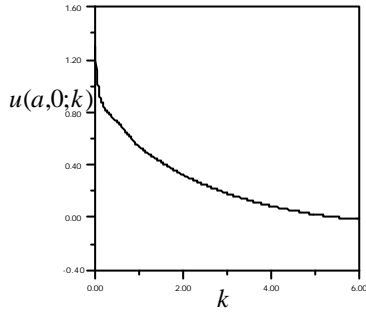


Fig.5 $u(a,0;k)$ versus k using
Burton and Miller method.

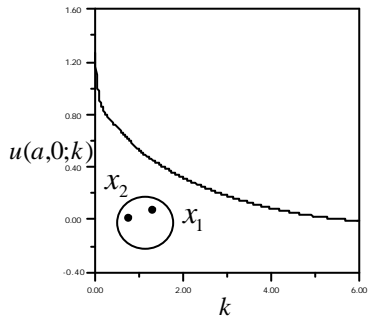


Fig.6 $u(a,0;k)$ versus k using
the CHIEF method

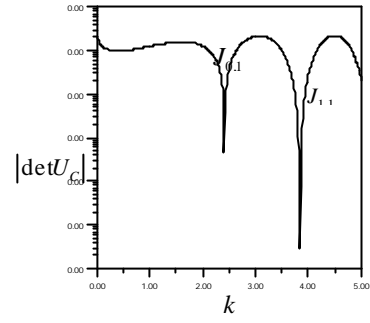


Fig.9 \mathbf{S}_1 versus k using
the complex BEM.

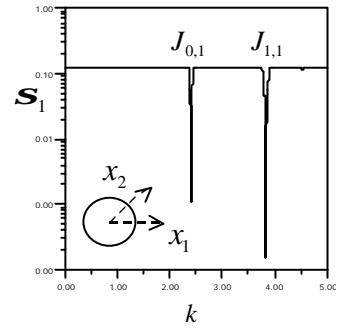


Fig.10 \mathbf{S}_1 versus k using
the CHIEF method

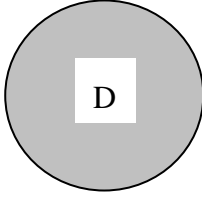
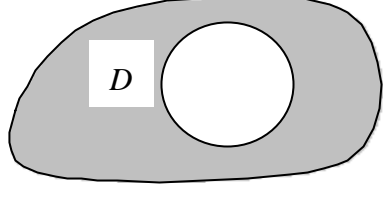
													
Method	Real-part BEM [16]		Imag.-part BEM [7,14]		Comp. BEM [4]		CHIEF BEM $\begin{bmatrix} G_{2N \times 2N}^B \\ G_a^e \end{bmatrix}$ [10]		Method	BEM [15]	BEM [15]	Burton & Miller [2]	CHIEF BEM $\begin{bmatrix} G_{2N \times 2N}^B \\ G_a^i \end{bmatrix}$ [1,11]
Equation	UT	LM	UT	LM	UT	LM	UT	LM	Equation	UT	LM	$UT + \frac{i}{k}LM$	UT or LM
Dirichlet B.C. analytical spurious solution	Y_n	Y'_n	J_n	J'_n	\times	\times	\times	\times	analytical fictitious solution	J_n	J'_n	\times	\times
Neumann B.C. analytical spurious solution	Y_n	Y'_n	J_n	J'_n	\times	\times	\times	\times	analytical fictitious solution	J_n	J'_n	\times	\times

Table 1. The relationship between spurious solution (interior problem) and fictitious solution (exterior problem).